2021-03-05

Ocean acidification increases phytobenthic carbon fixation and export in a warm-temperate system

Wada, S

10.1016/j.ecss.2020.107113
Estuarine, Coastal and Shelf Science
Elsevier BV

Ocean acidification increases phytobenthic carbon fixation and export in a warm-temperate system

Shigeki Wada[a*], Sylvain Agostini[a], Ben P. Harvey[a], Yuko Omori[b], Jason M. Hall-Spencer[a,c]

[a]Shimoda Marine Research Center, University of Tsukuba, Shimoda, Japan

[b]Life and Environmental Sciences, University of Tsukuba, Tsukuba, Japan

[c]School of Biological and Marine Sciences, University of Plymouth, Plymouth, UK

[*]Corresponding author: Shimoda Marine Research Center, University of Tsukuba, Shimoda, Shizuoka 415-0025, Japan

E-mail address: swadasbm@shimoda.tsukuba.ac.jp

1. ABSTRACT

The response of photosynthetic organisms to rising CO_2 levels is a key topic in ocean acidification research. Most of the work in this field has focused on physiological responses in laboratory conditions which lack ecological realism. Studies using seeps as natural analogues for ocean acidification have demonstrated shifts in algal community composition, but the effect of CO_2 on carbon fixation and export remains unclear. Here, we deployed artificial substrata in a warm-temperate region of Japan to collect algal communities using a CO_2 seep off Shikine Island. Diatoms became dominant on settlement substrata in areas with elevated CO_2 levels, whereas macroalgae dominated at present-day levels of CO_2 (reference site). This was supported by pigment composition; fucoxanthin content, characteristic of diatoms, was higher at the high CO_2 site, while more Chlorophyll *b,* which is characteristic of Chlorophyta, was found in the reference site. Algal communities that recruited in water with high levels of CO_2 had elevated rates of photosynthesis. Algal biomass was similar on all settlement panels, regardless of CO_2 concentration. Much of the carbon that was fixed by algae in the high CO_2 conditions was exported, likely due to detachment from the substratum. Diatoms that dominated under high CO_2 conditions are more easily transported away as they have no holdfast, whereas newly settled macroalgae became firmly attached at present-day levels of CO_2. These results show that ocean acidification may fundamentally alter coastal carbon cycling, increasing photosynthesis and carbon export from coastal ecosystems in warm-temperate biogeographic regions due to a shift in community composition from perennial to ephemeral algae.

Keywords: Carbon cycle, CO_2 seep, diatoms, macroalgae, marine productivity.

2. Introduction

Benthic algae are the major primary producers in shallow coastal regions (Charpy-Roubaud and Sournia, 1990), and they have a number of other important ecological roles such as a source of energy, carbon storage and habitat provisioning (Smale et al., 2013; Costanza et al., 2014). Recent work has shown that rising carbon dioxide levels influence these functions (Hall-Spencer and Harvey, 2019). Uptake of anthropogenic CO_2 is causing surface ocean seawater pH to fall by around 0.002 units per year with a 100% increase in the concentration of H^+ ions projected for the end of this century (IPCC, 2013). Ocean acidification is a serious threat to coastal ecosystems because it reduces the saturation state of carbonate which can make seawater corrosive to calcifying organisms such as hard corals and shellfish (Doney et al., 2020).

As well as reducing the availability of calcium carbonate, ocean acidification increases the amount of dissolved inorganic carbon (DIC) and this can stimulate the growth of certain photosynthetic organisms (Hendriks et al., 2010; Olischläger and Wiencke, 2013), if sufficient nutrients are available (Celis-Plá et al., 2015). Many algae benefit from increased seawater CO_2 concentrations in laboratory tests (Gao et al., 1991; Kubler et al., 1999; Liu et al., 2018) although the response is species-specific because some algae have carbon concentrating mechanisms (CCM) adapted to present day low CO_2 conditions (Badger et al., 1998; Cornwall et al., 2017).

To assess changes to coastal carbon cycling, we need to consider both the physiological responses of algae to ocean acidification, and the changes in community composition. In areas where CO_2 is released from volcanic seeps the gas dissolves into seawater providing a natural analogue for the effects of ocean acidification (Hall-Spencer et al., 2008) which include profound changes to benthic microalgal (Johnson et al., 2013)

and macroalgal communities at both individual and population levels (Porzio et al., 2011, 2018, 2020). At a recently characterised natural analogue site in Japan, calcifying algae and large habitat-forming macroalgae get replaced by turf algae at elevated CO_2 levels (Agostini et al., 2015, 2018; Harvey et al., 2019). This has been observed at many other shallow-water CO_2 seeps worldwide, although at some seeps seagrasses grow well (Hall-Spencer et al., 2008; Connell et al., 2018). In the present study, we assess how a CO_2 gradient at a Japanese seep affects algal community composition, photosynthesis and biomass production.

Measurements of photosynthesis at CO_2 seeps allow us to better constrain projections of the response of primary producers to ocean acidification. In addition, comparison of photosynthesis and biomass production furthers our understanding of carbon storage by coastal ecosystems. Previous studies taking this approach have assessed specific algal taxa (Hofmann et al., 2015; Vogel et al., 2015; Connell et al., 2018), but the effects of ocean acidification on benthic algal community photosynthesis had not previously been investigated. To tackle this, we used settlement panels which are widely used to easily collect natural benthic communities (Perkol-Finkel et al., 2006; Sokołowski et al., 2017). This technique has been used to assess shifts in benthic community composition along CO_2 gradients in the Mediterranean (Lidbury et al., 2012; Johnson et al., 2013; Kroeker et al., 2013b). Moreover, settlement panels also allow the investigation of the abundance, diversity and production of those communities of organisms that recruit on to them.

In the present study, we investigated high CO_2 and present-day conditions off Shikine Island, Japan. After 44 and 72 days we collected algal communities that had recruited *in situ*, recorded differences in community composition, incubated them in light

94 conditions to measure net photosynthesis, and then analysed the photosynthetic pigments
95 present. Our aim was to assess how high CO_2 conditions affect coastal carbon fixation
96 and storage.

3. Materials and methods

3.1. Study sites

We deployed algal settlement panels in and away from a CO_2 seep that is well characterised as an analogue for ocean acidification (Agostini et al., 2015, 2018). It is located off Mikawa Bay, Shikine Island (139.2°N, 34.3°E) in Japan (Fig. 1). Two sites were used, an acidified area near to the CO_2 seep (the 'high CO_2 site') and a nearby area (the 'reference site') in an adjacent bay of the island. The high CO_2 site provided an end-of-the-century projection for reductions in pH (IPCC, 2013), and was not confounded by differences in temperature, salinity, dissolved oxygen, total alkalinity, nutrients or depth relative to the reference site (Agostini et al., 2015, 2018; Harvey et al., 2019). Agostini et al. (2018) and Harvey et al. (2018) present the environmental and carbonate chemistry data collected during the present study. Briefly, seawater pH in total scale (pH_T) and other environmental parameters were monitored using a combination of sensors (interval of measurement was 15 or 30 min, recorded from 25th May to July 5th 2016) and discrete water sampling for total alkalinity. For reference and high CO_2 sites, pH_T was 8.137 ± 0.056 and 7.809 ± 0.093 respectively, the salinity was 34.5 ± 0.43 and 34.1 ± 0.69, the temperature was 19.7 ± 0.71 and 19.5 ± 0.82 °C, the total alkalinity was 2270 ± 15.4 and 2270 ± 20.3 μmol kg^{-1} and the calculated pCO_2 levels were 309 ± 46.4 and 769 ± 225 μatm (mean ± SD).

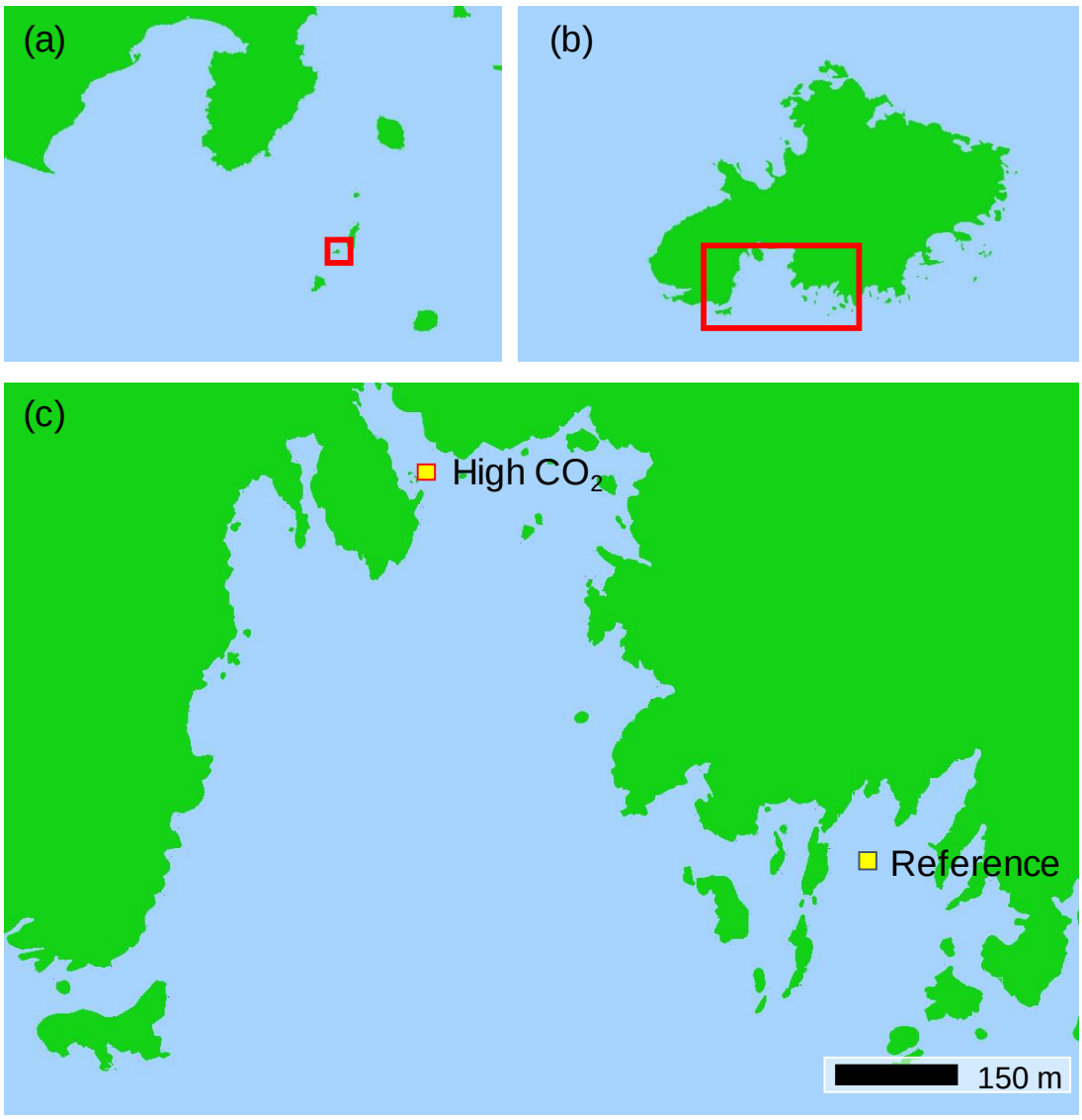

Figure 1. Study area off the Izu peninsula and archipelago off mainland Japan (a), Shikine Island (b) and the locations for the reference and high CO_2 site used for the deployment of settlement panels (c), land shown in green.

3.2. Deployment of settlement panels

Settlement panels were held at -5 m depth Chart Datum within the high CO_2 and reference sites. The panels were made of transparent PVC measuring 5×2×0.2 cm. A total of 76 panels were attached to floats anchored 1 m above the seafloor and haphazardly spread over a surface of ca. 400 m^2 in each site. In April 2016, we put four and five floats

123 in the high CO_2 and reference sites, respectively, corresponding to 34 panels in the high
124 CO_2 and 42 panels in the reference sites. Subsets of the panels were retrieved in June after
125 44 days and July (after 72 days). The algae on the panels were examined using a light
126 microscope.
127
128 **3.3. Pigment analysis**
129 After 44 and 72 days of deployment, 19 and 5 panels from the high CO_2, and 18 and
130 12 panels from the reference site were retrieved (at random) for pigment analysis. Each
131 settlement panel was photographed and analysed with imaging software (Adobe,
132 Photoshop) to measure the area size of the panels, and then stored at -80°C for pigment
133 analysis. The surface of each panel was scraped clean and the settled organisms were put
134 into 8 ml N'N-dimethylformamide to extract photosynthetic pigments. Canthaxanthin
135 was added to the extracts as an internal standard, and this was then filtered through a
136 polytetrafluorethylene (PTFE) filter with pore size of 0.45 μm (GE Healthcare Life
137 Science, Whatman™ syringe filter, 13 mm diameter). Aliquot of extracts was injected
138 into an isocratic high-performance liquid chromatograph (Agilent, 1100 system
139 controlled by ChemStation) equipped with a C8 column (Agilent, Zorbax Eclipse XDB-
140 C8; 4.6 × 150 mm, 3.5 μm) and diode-array and fluorescent detectors. The peak of each
141 pigment was identified by comparison of their retention time relative to eight standards;
142 fucoxanthin, prasinoxanthin, 19'-hexanoloxyfucoxanthin, diadinoxanthin, alloxanthin,
143 zeaxanthin, Chlorophyll *b* and Chlorophyll *a* (Chl *a*), as described in more detail in Hama
144 et al. (2016).
145
146 **3.4. Net photosynthesis**

147 After 44 and 72 days of deployment, 6 and 4 panels from the high CO_2, and 6 and 6
148 panels from the reference site were retrieved (at random) for the measurement of net
149 photosynthesis (NP). Incubation was carried out using a 250 ml acid-cleaned
150 polycarbonate bottle, with a subset of each panel (0.8 ×2.5 cm) being used. Each bottle
151 was filled with seawater collected from the site where the panels were retrieved, and
152 incubated under light (150 μmol photon s^{-1} cm^{-2}) at 20°C for 1 hr to measure rates of NP.
153 Dissolved oxygen (DO) concentrations and pH in NBS scale (pH_{NBS}) were measured at
154 the start and end of the incubation period with an optode DO meter (WTW, FD0925) and
155 a multi-sensor (ThermoFisher Scientific, Orion StarTM, equipped with a ROSS pH
156 electrode, 8156BNUWP). Based on the change in DO concentrations (ΔDO) values, we
157 calculated the NP rates (normalised by unit area) using the following equations:
158
159 NP_{area} (NP per unit area: μg O_2 cm^{-2} hour $^{-1}$) = $\Delta DO \times V / A / T \times 1000$
160 where V, A and T are volume of seawater for incubation (l), area of the plate (cm^2),
161 and incubation time (hour), respectively (Roth et al., 2019).
162
163 Following the incubation, each settlement panel was photographed and analysed
164 with imaging software (Adobe, Photoshop) to measure the exact panel area size. All
165 incubations were completed within 6 hrs of collecting the panels.
166
167 **3.5. Statistical analysis**
168 The amount of Chl *a* and the rates of NP_{area} were analysed using a two-way linear
169 mixed model (LMM) (R package: nlme, function: lme; *v3.1-147*: Pinheiro et al., 2020)
170 with 'Site' and 'Days' as fixed factors. Since several panels were attached to each float,

171 'float' was treated as a random factor. Homogeneity of variance (Levene Test) and
172 normality (QQ plot) were assessed for Chl *a* and NP_{area}. Both Chl *a* (following log
173 transformation) and NP_{area} conformed to these assumptions. Weighted principal
174 component analysis (R package: aroma light, functions: wpca: Bengtsson et al., 2010),
175 followed by PERMANOVA (R package: vegan, function: adonis; *v2.5-6*: Oksanen et al.,
176 2019), were used to assess for differences in the composition of accessory pigments
177 between 'Site' and 'Days'. Weighting for the principal component analysis was used to
178 improve the robustness to uneven group sample sizes, with weighting applied to each
179 sample individually as 1 / n, where n is the sample size of the respective treatment groups
180 (combinations of 'Site' and 'Days'). In the present study, all statistical analyses were
181 performed using the R statistical software, version 3.5.1 (R Core Team, 2018), and
182 visualisations were produced using ggplot 2 (Wickham, 2016) and ggpubr (Kassambara,
183 2020).

4. Results

Visual inspection of the panels revealed biofilm formation and algal recruitment on all panels across both sites and time points. At the high CO_2 site, the panel were covered with a homogenous brown biofilm at both time points (Fig. 2a,b). Panels at the reference site were covered with a more diverse range of algal recruits (Fig. 2c,d). After 72 days, the panels were more overgrown relative to 44 days, with juvenile macroalgal Chlorophyta dominating panels at the reference site whereas the diatoms *Triceratium* sp. and *Biddulphia* sp. were dominant on settlement panels at the high CO_2 site (Fig. 2e-g).

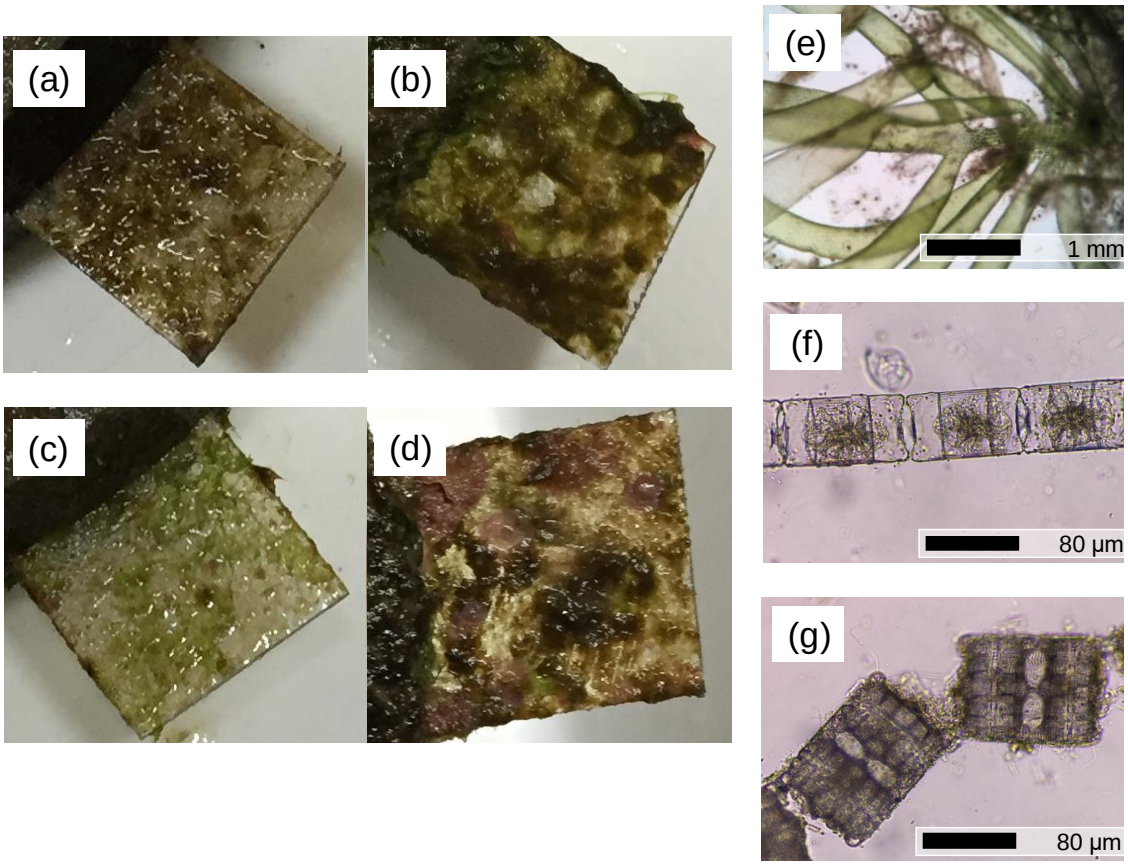

Figure 2. Panels retrieved from high CO_2 (a and b on day 44 and 72) and reference sites (c and d on day 44 and 72). Macroalgae dominated on settlement panels at the reference site (e), diatoms dominated at the acidified site; *Triceratium* sp. (f) and *Biddulphia* sp. (g).

Chl *a* was the main pigment and accounted for 31-68% of the total weight of

pigments per sample. The amount of Chl *a* per unit area of the plates deployed in the high CO_2 and reference sites was 0.284 ± 0.048 µg cm^{-2} and 0.285 ± 0.022 and on day 44, and increased to 1.86 ± 0.27 µg cm^{-2} and 2.03 ± 0.13 and on day 72, respectively (Fig. 3). While Chl *a* value significantly increased from day 44 to 72 (LMM, 'Days': $F_{1,5} = 93.49$, $p < 0.001$), there was no significant difference between the two sites (LMM, 'Site' x 'Days', $F_{1,5} = 4.68$, $p = 0.083$) (Table S1). Fucoxanthin was the second most abundant pigment, and the ratios of Fuc/Chl *a* on the panels from high CO_2 site were 1.01 ± 0.082 (n = 18) and 0.488 ± 0.041 (n = 5) on day 44 and 72, respectively. These values were relatively higher than those from reference site (0.724 ± 0.036 (n = 16) and 0.485 ± 0.070 (n = 12) on day 44 and 72, respectively).

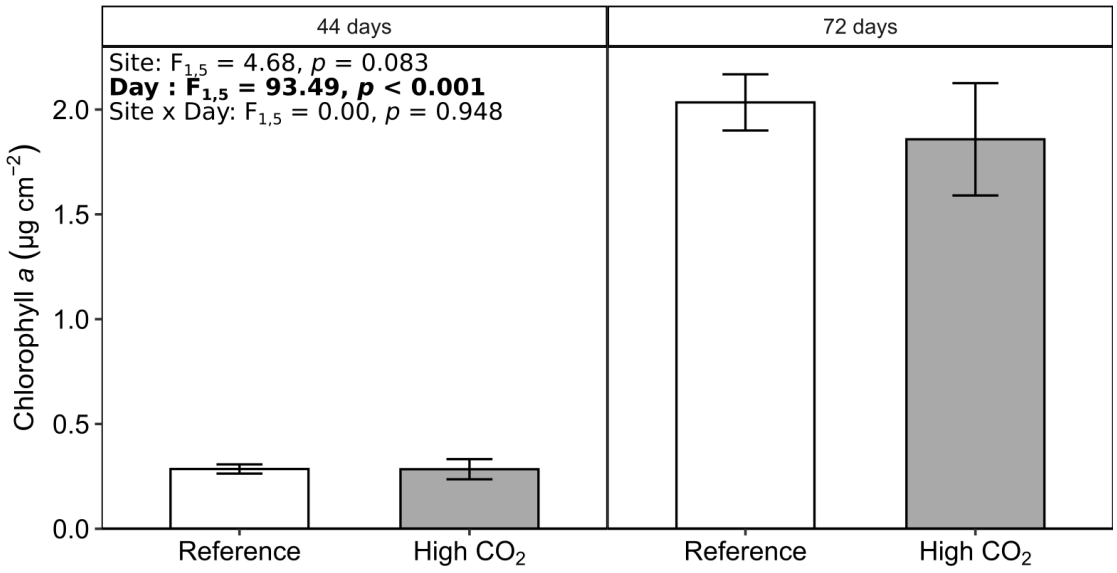

Figure 3. Mean Chlorophyll *a* per unit area of the panels (µg cm^{-2}) of panels at Reference (white) and High CO_2 (grey) sites after 44 and 72 days. Error bars show standard error (n = 18, 18, 12, 5). The statistical significance (linear mixed model on log-transformed data) of the main effects (Day and Site) and their interaction is shown.

The overall composition of the pigments differed between both the 'Site' (PERMANOVA: $F_{1, 47} = 27.44$, $p < 0.001$) and 'Days' (PERMANOVA: $F_{1, 47} = 13.22$, p

205 < 0.001), but did not show a significant interaction (PERMANOVA: $F_{1, 47} = 1.92$, $p =$
206 0.16) (Table S2). Principal component analysis showed that the two sites (high CO_2 and
207 reference) were mostly separated along PC1 (accounting for 28.8% of total variance; Fig.
208 S1) with values in a negative and positive direction distinguishing the high CO_2 and
209 reference sites, respectively (Fig. 4). The pigment fucoxanthin showed a loading of -0.55
210 on the PC1 and therefore had a moderate contribution towards explaining the high CO_2
211 site (Table 1). Chl *b* showed a positive loading of 0.70 and therefore had a moderate
212 contribution towards explaining the reference site (Table 1). The proportion of
213 fucoxanthin among accessory pigments were generally higher at the high CO_2 site
214 compared to the reference site, whereas the proportion of chlorophyll *b* was higher in the
215 reference site, and below detection limit at day 44 in the High CO_2 site (Table 1). The two
216 'Days' (44 and 72) were mostly separated along PC2 (accounting for 20.1% of total
217 variance; Fig. S1) with values in a negative and positive direction distinguishing the
218 earlier (day 44) and latter (day 72) sampling points, respectively (Fig. 4). Prasinoxanthin,
219 diadinoxanthin, and 19'-hexanoloxyfucoxanthin had a moderate contribution (-0.70, -
220 0.53 and -0.31, respectively) towards explaining the earlier and latter sampling points
221 (Table 1). Of these pigments, diadinoxanthin represented between 9-19% of the total
222 accessories pigments, although the other two pigments (Prasinoxanthin and 19'-
223 hexanoloxyfucoxanthin) represented less than 5% (Table 1). The two other pigments,
224 Alloxanthin and Zeaxanthin were minor components, contributing less than 4.2% each to
225 the total accessory pigments (Table 1).

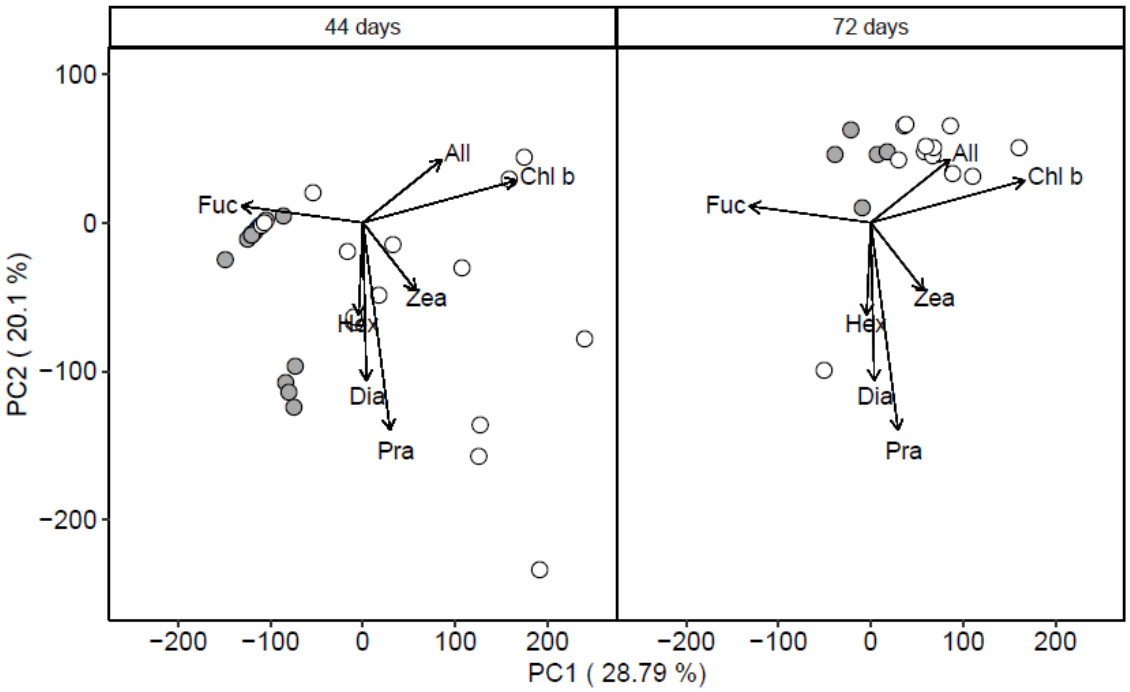

Figure 4. Weighted principal component analysis biplot of accessory pigments across site (High CO_2, filled circles, Reference - empty circles) and time points (44 days - left, and 72 days - right). The same PCA is used for both panels, but time points were separated for ease of visualisation, with the loading of each pigment indicated by vectors. The accessory pigments are fucoxanthin (Fuc), prasinoxanthin (Pra), 19'-hexanoloxyfucoxanthin (Hex), diadinoxanthin (Dia), alloxanthin (All), zeaxanthin (Zea) and chlorophyll *b* (Chl *b*).

226

Table 1. PCA loadings of the different pigments (across both sites and time points), and their percentage weights (mean ± se (n)) for each site and time point.

			Percentage Weight			
	PCA loading		44 days after		72 days after	
Pigment	PC1	PC2	Reference	High CO_2	Reference	High CO_2
Alloxanthin	0.36	0.21	1.8 ± 0.5 (16)	0.2 ± 0.2 (18)	1.2 ± 0.2 (12)	2.1 ± 0.1 (5)
Chlorophyll *b*	0.70	0.14	7.1 ± 2 (16)	0 ± 0 (18)	7.8 ± 1.1 (12)	2.9 ± 1.2 (5)
Diadinoxanthin	0.02	-0.53	12.4 ± 0.3 (16)	14.9 ± 0.3 (18)	11.7 ± 0.4 (12)	12.4 ± 0.6 (5)

Fucoxanthin	-0.55	0.06	72.8 ± 2.4 (16)	84 ± 0.4 (18)	72.9 ± 1 (12)	79.3 ± 1.4 (5)
19'-Hexanoloxyfucoxanthin	0.02	-0.31	0.8 ± 0.6 (16)	0 ± 0 (18)	5 ± 0.6 (12)	3.1 ± 0.3 (5)
Prasinoxanthin	0.12	-0.70	0.9 ± 0.5 (16)	0.9 ± 0.4 (18)	0.3 ± 0.3 (12)	0 ± 0 (5)
Zeaxanthin	0.24	-0.23	4.2 ± 0.7 (16)	0 ± 0 (18)	1.1 ± 0.3 (12)	0.2 ± 0.2 (5)

The pH_{NBS} values of the seawater collected from the high CO_2 and reference sites (at 20°C) were 7.92 ± 0.003 and 8.20 ± 0.006 on day 44, and 7.70 ± 0.009 and 8.16 ± 0.007 (mean ± SD) on day 72, respectively. The changes in pH_{NBS} (ΔpH_{NBS}) under light incubation for the sample from high CO_2 and reference sites were 0.068 ± 0.007 and 0.043 ± 0.008 on day 44, and 0.046 ± 0.020 and 0.052 ± 0.006 (mean ± SD) on day 72, respectively, reflecting CO_2 consumption by photosynthesis. Since the changes in the pH_{NBS} during the incubations were within narrow ranges (from 0.023 to 0.081), differences in pH_{NBS} between the seawater collected from the high CO_2 and reference sites were maintained throughout the experiment. The concentrations of DO at the start of light incubations were 8.73 - 9.48 mg l^{-1}, and changes in the incubation period were 0.18 - 0.93 mg l^{-1}.

Net photosynthesis rates (NP_{area}) of the panels from the high CO_2 site were 16.5 ± 1.3 (mean ± SE, n = 6) and 31.7 ± 1.8 (mean ± SE, n = 4) μg O_2 cm^{-2} $hour^{-1}$ on day 44 and 72, and from the reference site were 6.94 ± 0.71, (mean ± SE, n = 6) and 21.8 ± 2.6, (mean ± SE, n = 6) μg O_2 cm^{-2} $hour^{-1}$ on day 44 and 72, respectively (Fig. 4). Overall, this meant that NP_{area} of the settlement panels was significantly greater on Day 72

244 compared to Day 44 (LMM: 'Day', $F_{1,5} = 34.29$, $p < 0.01$), and also higher at the high

245 CO_2 site relative to the reference site (LMM: 'Site', $F_{1,5} = 10.41$, $p < 0.05$) (Fig. 5, Table

246 S3).

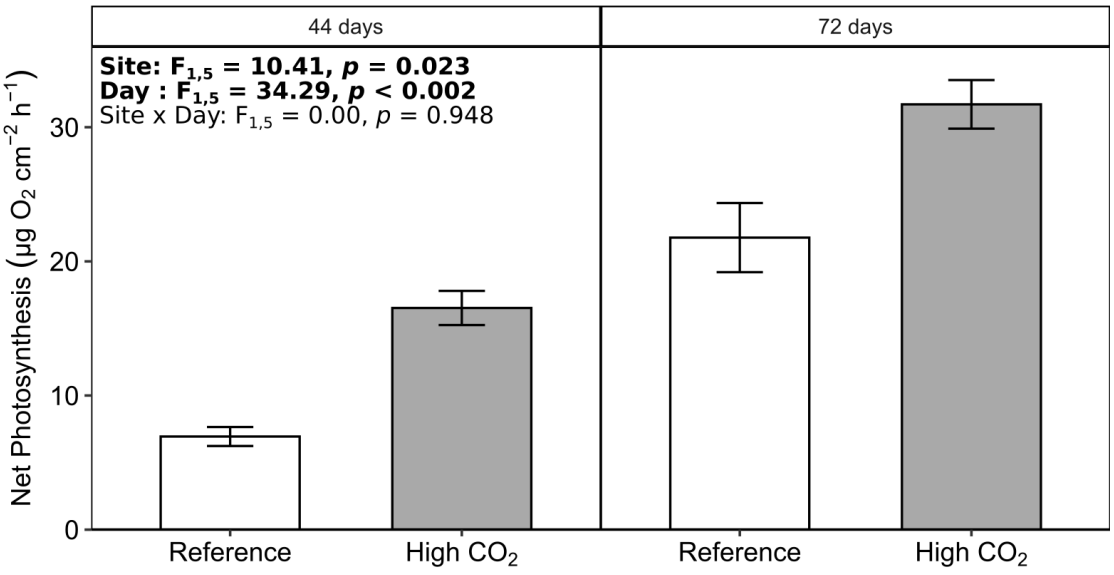

Figure 5. Net photosynthic rates during laboratory incubation of panels from Reference (white bars) and High CO_2 (grey bars) sites and time points (44 and 72 days) in seawater sampled at the same site. Error bars show standard error (n = 6, 6, 6, 4, respectively). The statistical significance (linear mixed model) of the main effects (Day and Site) and their interaction is shown.

247

5. Discussion

Studies of carbon dioxide seeps worldwide have shown that increasing levels of ocean acidification cause major shifts in coastal algal community composition (Hall-Spencer and Harvey, 2019). Here we show that algal settlement is affected by increasing levels of CO_2. Macroalgal recruits dominated settlement panels at a reference site, being well attached by holdfasts, whereas less firmly attached diatoms dominated on panels at a high CO_2 site (Fig. 2). The differences in algal communities were confirmed through photosynthetic pigment analysis. The amount of fucoxanthins was higher in the algal communities at high CO_2, these pigments are common in heterokont algae such as diatoms and brown algae (Dring, 1998; Kuczynska et al., 2015).

Microscopy showed that diatoms, rather than brown algae, dominated the early stages of settlement at high CO_2, and this was confirmed by our pigment analyses after 44 and 72 days of settlement on panels. The pigment composition of brown algae and benthic diatom mats reported in previous studies show that the ratio of Fuc/Chl *a* in most brown algae (mean values among 30 species: 0.372; Colombo-Pallotta et al., 2006; Desmond et al., 2019; Marambio et al., 2017; Seely et al., 1972; Verma et al., 2017) were lower than those of natural diatom mats (mean values among 4 reports: 1.168; Sundback et al. 1996; Wulff et al. 2005; 2008; Stief et al. 2013) (Table S4). Considering the higher ratio of Fuc/Chl *a* on the panels from the high CO_2 site, this confirms that benthic diatoms were dominant at the high CO_2 site. In contrast, there was significantly more Chl *b* in the algal community that settled onto the Reference site panels (Table 1), and this is the main accessory pigment of Chlorophyta (Dring, 1998). Studies worldwide show that benthic diatoms seem to be capable of benefitting from ocean acidification/high CO_2 conditions (Johnson et al., 2013; Marques da Silva et al., 2017; Harvey et al., 2019). Deployment of

272 settlement panels at this site showed that diatom recruitment was more intense in the high
273 CO_2 site than in reference conditions.

274 Our study sites off Shikine island were very exposed to wave action and are in the
275 path of a strong ocean current (Kuroshio current), so it is worth comparing our results
276 with those from experiments set up in more sheltered conditions. Recruitment of algae
277 using artificial substrata have been assessed at CO_2 seeps off the islands of Vulcano and
278 Ischia in Italy which are both less exposed to strong water movement than Shikine Island.
279 Off Vulcano, Johnson et al. (2013) also found higher diatom abundance at high CO_2 on
280 settlement substrata suspended in the water column, but did not report on export of the
281 biomass grown in these conditions. Off Ischia island CO_2 seeps, volcanic stone tiles were
282 attached to the seafloor to monitor algal succession for 2-14 months (Kroeker et al. 2012;
283 Porzio et al. 2013). Contrary to the present study, only a minimal biomass of diatoms was
284 reported at high CO_2. As the panels in the present study were suspended off the seafloor,
285 benthic herbivores, such as gastropods, did not have access to the floats to graze. Since
286 grazing pressure is an important driving force in the community composition of benthic
287 flora (Hillebrand et al. 2000), the deployment position of the artificial substrata
288 (suspended or attached) could lead to differences in successional processes. In addition
289 to the environmental condition and experimental set-up, the duration of the experimental
290 deployment represents another important factor determining algal community succession.
291 Our experiment examined the phase of early succession, so there is scope in future studies
292 to investigate the effects of ocean acidification on the long-term development of
293 biofouling communities as it takes many months for these communities to mature
294 (Kroeker et al., 2013b; Brown et al., 2018).

295 Net photosynthetic rates were significantly higher on the high CO_2 panels than on

296 the Reference panels (Fig. 5, Table S3), showing an increase in carbon fixation under
297 ocean acidification. In the present day, CO_2 concentrations in surface seawater are
298 generally less than 15 μmol kg^{-1} (Zeebe and Wolf-Gladrow, 2009) which can limit
299 photosynthetic rates, through substrate limitation (Badger et al., 1998). Previous
300 laboratory and aquarium-based studies have shown that increased CO_2 can enhance
301 photosynthesis in some algae (Gao et al., 1991; Kubler et al., 1999; Liu et al., 2018).
302 However, a number of recent studies have found that increased CO_2 can have no or even
303 negative effects on photosynthesis in several algal species (Peach et al. 2017; Porzio et al.
304 2020), highlighting that responses to ocean acidification are species-specific. These
305 interspecific differences lead to shifts in community composition under high CO_2
306 conditions, which complicates the up-scaling of laboratory studies to ecosystem-level
307 change. In the present study, we demonstrate that *in situ* photosynthesis of an algal
308 community increased with ocean acidification, which is directly relevant for future
309 projections of primary production and carbon storage.

310 Although algal community productivity was enhanced in high-CO_2 conditions, the
311 Chl *a* content on these settlement panels was similar to those in reference site conditions
312 (Fig. 3) showing that algal biomass did not increase despite enhanced photosynthesis.
313 This mismatch between photosynthesis and biomass suggests that a large part of the fixed
314 carbon was subsequently being lost in the high-CO_2 conditions due to the detachment of
315 algae and export of carbon from the substratum. In the reference site, macroalgae were
316 held in place by holdfasts which strongly attached the thalli to hard surfaces and helped
317 them resist drag forces due to waves and currents. Diatoms, which were dominant on the
318 panels in the high CO_2 site, have no holdfast and are only attached by sticky mucus
319 materials exuded extracellularly (Hoagland et al., 1993). At our seep site, benthic diatoms

were so abundant that they formed turf-like mats in areas with high CO_2 (Fig. S2a and Agostini et al., 2018; Harvey et al., 2019). Detached aggregations of these turf diatoms at the high CO_2 site occur during the spring-summer season, where they can be seen drifting in clumps across the seabed (Fig. S2b,c). The drifting algal aggregates are typically a mixture of diatom and drift macroalgae, with the diatom species identified on the panels (*Triceratium* sp. and *Biddulphia* sp.) found in large numbers within the aggregates (Fig. S2d,e).

Our findings support other research showing that ocean acidification changes coastal algal communities, and we provide novel data showing its effects on coastal carbon fixation and export. Although algae will continue to provide a huge amount of energy for coastal ecosystems through high rates of photosynthesis (Mann, 1973; Graham et al., 2016), our data show a shift from resilient, long-lived, diverse algal stands that store large amounts of carbon, to less resilient, short-lived and less diverse stands that have increased rates of carbon fixation but greater rates of carbon export. Such changes in algal communities reduce habitat complexity and algal biomass in rocky shore habitats. Unless humanity is able to minimize and address the impacts of ocean acidification we can expect that it will cause major disruption to coastal ecosystems with knock-on effects on nearshore food webs, fisheries and carbon cycle.

6. Acknowledgements

We thank the technical staff of Shimoda Marine Research Center and Mr Yasutaka Tsuchiya, for help with field sampling. We are also grateful to Dr T. Hama for his kind advice. The species identification of diatoms was supported by Drs K. Ishida and T. Nakayama. Dr J. Hama helped with HPLC analysis. The field survey was permitted by

Nii-jima Fishery Cooperatives Shikine-jima Branch. This study was supported by the Environment Research and Technology Development Fund (4RF-1701), the Ministry of Education, Science, Sports and Culture, Grant-in-Aid for Scientific Research (B) (19H04234) and Graind-in-Aid for Young Scientists (B) (17K17622), and the International Educational and Research Laboratory Program of the University of Tsukuba.

7. References

Agostini, S., Harvey, B.P., Wada, S., Kon, K., Milazzo, M., Inaba, K., Hall-Spencer, J.M., 2018. Ocean acidification drives community shifts towards simplified non-calcified habitats in a subtropical−temperate transition zone. Scientific Reports 8. https://doi.org/10.1038/s41598-018-29251-7

Agostini, S., Wada, S., Kon, K., Omori, A., Kohtsuka, H., Fujimura, H., Tsuchiya, Y., Sato, T., Shinagawa, H., Yamada, Y., Inaba, K., 2015. Geochemistry of two shallow CO_2 seeps in Shikine Island (Japan) and their potential for ocean acidification research. Regional Studies in Marine Science 2, 45–53. https://doi.org/10.1016/j.rsma.2015.07.004

Azevedo, L.B., De Schryver, A.M., Hendriks, A.J., Huijbregts, M.A.J., 2015. Calcifying Species Sensitivity Distributions for Ocean Acidification. Environmental Science & Technology 49, 1495–1500. https://doi.org/10.1021/es505485m

Badger, M.R., Andrews, T.J., Whitney, S.M., Ludwig, M., Yellowlees, D.C., Leggat, W., Price, G.D., 1998. The diversity and coevolution of Rubisco, plastids, pyrenoids, and chloroplast-based CO_2 -concentrating mechanisms in algae. Canadian Journal of Botany 76, 1052–1071. https://doi.org/10.1139/b98-074

Bengtsson, H., Neuvial, P., Speed, T.P., 2010. TumorBoost: Normalization of allele-specific tumor copy numbers from a single pair of tumor-normal genotyping microarrays. BMC Bioinformatics 11, 245. https://doi.org/10.1186/1471-2105-11-245

Brown, N.E.M., Milazzo, M., Rastrick, S.P.S., Hall-Spencer, J.M., Therriault, T.W., Harley, C.D.G., 2018. Natural acidification changes the timing and rate of succession, alters community structure, and increases homogeneity in marine biofouling communities. Global Change Biology 24, e112–e127. https://doi.org/10.1111/gcb.13856

Celis-Plá, P.S.M., Hall-Spencer, J.M., Horta, P.A., Milazzo, M., Korbee, N., Cornwall, C.E., Figueroa, F.L., 2015. Macroalgal responses to ocean acidification depend on nutrient and light levels. Frontiers in Marine Science 2. https://doi.org/10.3389/fmars.2015.00026

Charpy-Roubaud, C., Sournia, A., 1990. The comparative estimation of phytoplanktonic, microphytobenthic and macrophytobenthic primary production in the oceans'. Marine Microbial Food Webs 4, 31–57.

Colombo-Pallotta, M.F., García-Mendoza, E., Ladah, L.B., 2006. Photosynthetic performance, light absorption, and pgiment composition of *Macrocystis pyrifera* (Laminariales, Phaeophyceae) blades from different depths. Journal of Phycology 42, 1225–1234. https://doi.org/10.1111/j.1529-8817.2006.00287.x

Connell, S.D., Doubleday, Z.A., Foster, N.R., Hamlyn, S.B., Harley, C.D.G., Helmuth, B., Kelaher, B.P., Nagelkerken, I., Rodgers, K.L., Sarà, G., Russell, B.D., 2018. The duality of ocean acidification as a resource and a stressor. Ecology 99, 1005–1010. https://doi.org/10.1002/ecy.2209

Cornwall, C.E., Revill, A.T., Hall-Spencer, J.M., Milazzo, M., Raven, J.A., Hurd, C.L., 2017. Inorganic carbon physiology underpins macroalgal responses to elevated CO_2. Scientific Reports 7. https://doi.org/10.1038/srep46297

Costanza, R., de Groot, R., Sutton, P., van der Ploeg, S., Anderson, S.J., Kubiszewski, I., Farber, S., Turner, R.K., 2014. Changes in the global value of ecosystem services. Global Environmental Change 26, 152–158.

https://doi.org/10.1016/j.gloenvcha.2014.04.002
Desmond, M.J., Pajusalu, L., Pritchard, D.W., Stephens, T.A., Hepburn, C.D., 2019. Whole community estimates of macroalgal pigment concentration within two southern New Zealand kelp forests. Journal of Phycology 55, 936–947. https://doi.org/10.1111/jpy.12884
Doney, S.C., Busch, D.S., Cooley, S.R., Kroeker, K.J., 2020. The Impacts of Ocean Acidification on Marine Ecosystems and Reliant Human Communities. Annual Review of Environment and Resources 45, 83–112. https://doi.org/10.1146/annurev-environ-012320-083019
Dring, M.J., 1998. The Biology of Marine Plants. Univ. Press, Cambridge.
Gao, K., Aruga, Y., Asada, K., Ishihara, T., Akano, T., Kiyohara, M., 1991. Enhanced growth of the red alga Porphyra yezoensis Ueda in high CO_2 concentrations. Journal of Applied Phycology 3, 355–362.
Graham, M., Fox, M., Hamilton, S., 2016. Macrophyte Productivity and the Provisioning of Energy and Habitat to Nearshore Systems, in: Ólafsson, E. (Ed.), Marine Macrophytes as Foundation Species. CRC Press, Taylor & Francis Group, 6000 Broken Sound Parkway NW, Suite 300, Boca Raton, FL 33487-2742, pp. 133–152. https://doi.org/10.4324/9781315370781-7
Hall-Spencer, J.M., Harvey, B.P., 2019. Ocean acidification impacts on coastal ecosystem services due to habitat degradation. Emerging Topics in Life Sciences 3, 197–206. https://doi.org/10.1042/ETLS20180117
Hall-Spencer, J.M., Rodolfo-Metalpa, R., Martin, S., Ransome, E., Fine, M., Turner, S.M., Rowley, S.J., Tedesco, D., Buia, M.-C., 2008. Volcanic carbon dioxide vents show ecosystem effects of ocean acidification. Nature 454, 96–99. https://doi.org/10.1038/nature07051
Hama, T., Inoue, T., Suzuki, R., Kashiwazaki, H., Wada, S., Sasano, D., Kosugi, N., Ishii, M., 2016. Response of a phytoplankton community to nutrient addition under different CO_2 and pH conditions. Journal of Oceanography 72, 207–223. https://doi.org/10.1007/s10872-015-0322-4
Harvey, B.P., Agostini, S., Kon, K., Wada, S., Hall-Spencer, J.M., 2019. Diatoms Dominate and Alter Marine Food-Webs When CO_2 Rises. Diversity 11, 242. https://doi.org/10.3390/d11120242
Harvey, B.P., Agostini, S., Wada, S., Inaba, K., Hall-Spencer, J.M., 2018. Dissolution: The Achilles' Heel of the Triton Shell in an Acidifying Ocean. Frontiers in Marine Science 5. https://doi.org/10.3389/fmars.2018.00371
Hendriks, I.E., Duarte, C.M., Álvarez, M., 2010. Vulnerability of marine biodiversity to ocean acidification: A meta-analysis. Estuarine, Coastal and Shelf Science 86, 157–164. https://doi.org/10.1016/j.ecss.2009.11.022
Hoagland, K.D., Rosowski, J.R., Gretz, M.R., Roemer, S.C., 1993. Diatom extracellular polymeric substances: function, fine structure, chemistry, and physiology. Journal of Phycology 29, 537–566. https://doi.org/10.1111/j.0022-3646.1993.00537.x
Hofmann, L.C., Fink, A., Bischof, K., de Beer, D., 2015. Microsensor studies on *Padina* from a natural CO_2 seep: implications of morphology on acclimation to low pH. Journal of Phycology 51, 1106–1115. https://doi.org/10.1111/jpy.12347
IPCC, 2013. Climate change 2013: The Physical Science Basis. Contribution of Working Group I to the Fifth Assessment Report of the Intergovernmental Panel on Climate Change. URL https://www.ipcc.ch/report/ar5/wg1/ (accessed 1.10.19).

Johnson, V.R., Brownlee, C., Rickaby, R.E.M., Graziano, M., Milazzo, M., Hall-Spencer, J.M., 2013. Responses of marine benthic microalgae to elevated CO_2. Marine Biology 160, 1813–1824. https://doi.org/10.1007/s00227-011-1840-2

Kassambara, A., 2020. ggpubr: "ggplot2" Based Publication Ready Plots.

Kroeker, K.J., Kordas, R.L., Crim, R., Hendriks, I.E., Ramajo, L., Singh, G.S., Duarte, C.M., Gattuso, J.-P., 2013a. Impacts of ocean acidification on marine organisms: quantifying sensitivities and interaction with warming. Global Change Biology 19, 1884–1896. https://doi.org/10.1111/gcb.12179

Kroeker, K.J., Micheli, F., Gambi, M.C., 2013b. Ocean acidification causes ecosystem shifts via altered competitive interactions. Nature Climate Change 3, 156–159. https://doi.org/10.1038/nclimate1680

Kubler, J.E., Johnston, A.M., Raven, J.A., 1999. The effects of reduced and elevated CO_2 and O_2 on the seaweed *Lomentaria articulata*. Plant, Cell and Environment 22, 1303–1310. https://doi.org/10.1046/j.1365-3040.1999.00492.x

Kuczynska, P., Jemiola-Rzeminska, M., Strzalka, K., 2015. Photosynthetic Pigments in Diatoms. Marine Drugs 13, 5847–5881. https://doi.org/10.3390/md13095847

Lidbury, I., Johnson, V., Hall-Spencer, J.M., Munn, C.B., Cunliffe, M., 2012. Community-level response of coastal microbial biofilms to ocean acidification in a natural carbon dioxide vent ecosystem. Marine Pollution Bulletin 64, 1063–1066. https://doi.org/10.1016/j.marpolbul.2012.02.011

Liu, L., Zou, D., Jiang, H., Chen, B., Zeng, X., 2018. Effects of increased CO_2 and temperature on the growth and photosynthesis in the marine macroalga Gracilaria lemaneiformis from the coastal waters of South China. Journal of Applied Phycology 30, 1271–1280. https://doi.org/10.1007/s10811-017-1316-y

Mann, K.H., 1973. Seaweeds: Their Productivity and Strategy for Growth: The role of large marine algae in coastal productivity is far more important than has been suspected. Science 182, 975–981. https://doi.org/10.1126/science.182.4116.975

Marambio, J., Rodriguez, J.P., Mendez, F., Ocaranza, P., Rosenfeld, S., Ojeda, J., Rautenberger, R., Bischof, K., Terrados, J., Mansilla, A., 2017. Photosynthetic performance and pigment composition of Macrocystis pyrifera (Laminariales, Phaeophyceae) along a gradient of depth and seasonality in the ecoregion of Magellan, Chile. Journal of Applied Phycology 29, 2575–2585. https://doi.org/10.1007/s10811-017-1136-0

Marques da Silva, J., Cruz, S., Cartaxana, P., 2017. Inorganic carbon availability in benthic diatom communities: photosynthesis and migration. Philosophical Transactions of the Royal Society B: Biological Sciences 372, 20160398. https://doi.org/10.1098/rstb.2016.0398

Méndez, F., Marambio, J., Ojeda, J., Rosenfeld, S., Rodríguez, J.P., Tala, F., Mansilla, A., 2019. Variation of the photosynthetic activity and pigment composition in two morphotypes of Durvillaea antarctica (Phaeophyceae) in the sub-Antarctic ecoregion of Magallanes, Chile. J Appl Phycol 31, 905–913. https://doi.org/10.1007/s10811-018-1675-z

Oksanen, J., Blanchet, F.G., Friendly, M., Kindt, R., Legendre, P., McGlinn, D., Minchin, P.R., O'Hara, R.B., Simpson, G.L., Solymos, P., Stevens, M.H.H., Szoecs, E., Wagner, H., 2019. vegan: Community Ecology Package.

Olischläger, M., Wiencke, C., 2013. Ocean acidification alleviates low-temperature effects on growth and photosynthesis of the red alga Neosiphonia harveyi

(Rhodophyta). Journal of Experimental Botany 64, 5587–5597. https://doi.org/10.1093/jxb/ert329

Perkol-Finkel, S., Zilman, G., Sella, I., Miloh, T., Benayahu, Y., 2006. Floating and fixed artificial habitats: effects of substratum motion on benthic communities in a coral reef environment. Marine Ecology Progress Series 317, 9–20. https://doi.org/10.3354/meps317009

Pinheiro, J., Bates, D., DebRoy, S., Sarkar, D., EISPACK, E., Heisterkamp, S., Willigen, B.V., R-core, 2020. nlme: Linear and Nonlinear Mixed Effects Models.

Porzio, L., Arena, C., Lorenti, M., De Maio, A., Buia, M.C., 2020. Long-term response of Dictyota dichotoma var. intricata (C. Agardh) Greville (Phaeophyceae) to ocean acidification: Insights from high pCO2 vents. Science of The Total Environment 731, 138896. https://doi.org/10.1016/j.scitotenv.2020.138896

Porzio, L., Buia, M.C., Ferretti, V., Lorenti, M., Rossi, M., Trifuoggi, M., Vergara, A., Arena, C., 2018. Photosynthesis and mineralogy of Jania rubens at low pH/high pCO2: A future perspective. Science of The Total Environment 628–629, 375–383. https://doi.org/10.1016/j.scitotenv.2018.02.065

Porzio, L., Buia, M.C., Hall-Spencer, J.M., 2011. Effects of ocean acidification on macroalgal communities. Journal of Experimental Marine Biology and Ecology 400, 278–287. https://doi.org/10.1016/j.jembe.2011.02.011

R Core Team, 2018. R: A Language and Environment for Statistical Computing. R Foundation for Statistical Computing, Vienna, Austria.

Roth, F., Wild, C., Carvalho, S., Rädecker, N., Voolstra, C.R., Kürten, B., Anlauf, H., El-Khaled, Y.C., Carolan, R., Jones, B.H., 2019. An in situ approach for measuring biogeochemical fluxes in structurally complex benthic communities. Methods in Ecology and Evolution 10, 712–725. https://doi.org/10.1111/2041-210X.13151

Seely, G.R., Duncan, M.J., Vidaver, W.E., 1972. Preparative and analytical extraction of pigments from brown algae with dimethyl sulfoxide. Marine Biology 12, 184–188. https://doi.org/10.1007/BF00350754

Smale, D.A., Burrows, M.T., Moore, P., O'Connor, N., Hawkins, S.J., 2013. Threats and knowledge gaps for ecosystem services provided by kelp forests: a northeast Atlantic perspective. Ecology and Evolution 3, 4016–4038. https://doi.org/10.1002/ece3.774

Sokołowski, A., Ziółkowska, M., Balazy, P., Kukliński, P., Plichta, I., 2017. Seasonal and multi-annual patterns of colonisation and growth of sessile benthic fauna on artificial substrates in the brackish low-diversity system of the Baltic Sea. Hydrobiologia 790, 183–200. https://doi.org/10.1007/s10750-016-3043-9

Verma, P., Kumar, M., Mishra, G., Sahoo, D., 2017. Multivariate analysis of fatty acid and biochemical constitutes of seaweeds to characterize their potential as bioresource for biofuel and fine chemicals. Bioresource Technology 226, 132–144. https://doi.org/10.1016/j.biortech.2016.11.044

Vogel, N., Fabricius, K.E., Strahl, J., Noonan, S.H.C., Wild, C., Uthicke, S., 2015. Calcareous green alga *Halimeda* tolerates ocean acidification conditions at tropical carbon dioxide seeps: *Halimeda* growing at CO_2 seeps. Limnology and Oceanography 60, 263–275. https://doi.org/10.1002/lno.10021

Waldbusser, G.G., Hales, B., Langdon, C.J., Haley, B.A., Schrader, P., Brunner, E.L., Gray, M.W., Miller, C.A., Gimenez, I., 2015. Saturation-state sensitivity of marine bivalve larvae to ocean acidification. Nature Climate Change 5, 273–280.

https://doi.org/10.1038/nclimate2479
Wickham, H., 2016. ggplot2: Elegant Graphics for Data Analysis. Springer-Verlag New York.
Zeebe, R.E., Wolf-Gladrow, D., 2009. CO_2 in Seawater: Equilibrium, Kinetics, Isotopes. Elsevier Oceanography Series 65.

Supporting Information

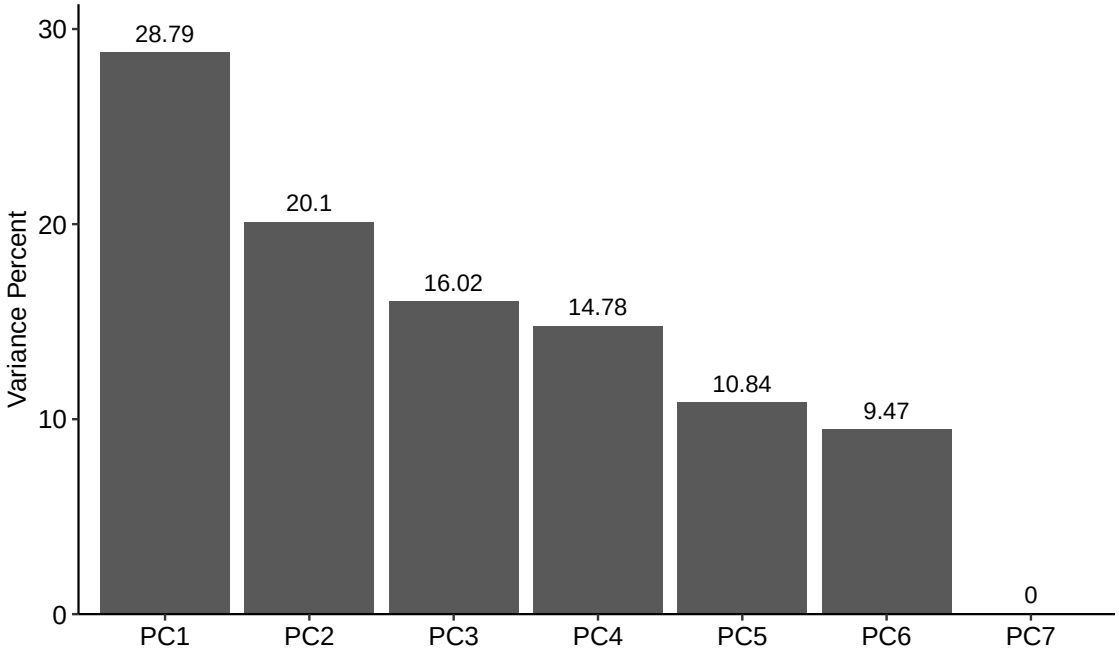

Figure S1. Scree plot for the weighted principal component analysis. Loadings of each component were shown in descending order. The ordinate and abscissa are percent value of variance and number of dimensions, respectively.

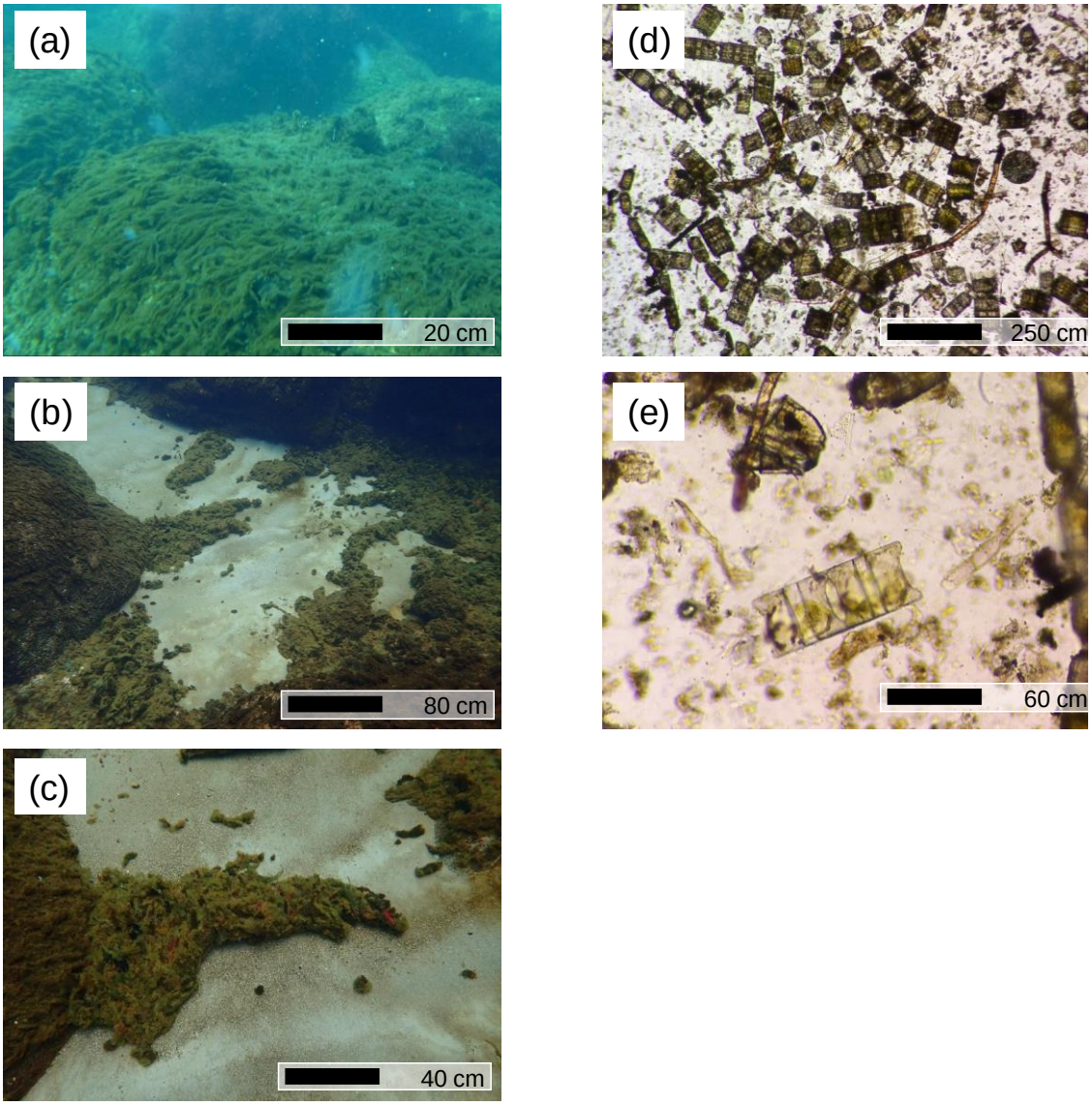

Figure S2. Photo's of a diatom mat found on rocks in a high CO_2 site (a), algae drifting near the high CO_2 site (b and c: zoomed out and in, respectively), and diatoms identified in the clumps (d and e: mainly *Biddulphia* sp. and *Triceratium* sp., respectively).

Table S1. ANOVA results of the linear mixed model for log transformed chlorophyll *a*. Degrees of freedom (df), F-values (F) and significance probability (Pr) were shown for main effects ('Site' and 'Days') and interaction.

	df	F	Pr(>F)
(Intercept)	1, 44	16.74	0.0002
Site	1, 5	4.68	0.0829
Days	1, 5	93.49	0.0002
Site:Days	1, 5	0.00	0.9997

Table S2. PERMANOVA table of the pigment composition (Bray Curtis distance). (999 permutations). Degrees of freedom (df), sum of squares (SumOfSqs), mean sum of squares (MeanSqs), F-statistic (F.Model), coefficients of determination (R^2) and significance probabilities (Pr) were shown.

	df	SumOfSqs	MeanSqs	F.Model	R^2	Pr(>F)
Days	1	0.076	0.076	13.217	0.148	0.001
Site	1	0.158	0.158	27.438	0.306	0.001
Days:Site	1	0.011	0.011	1.920	0.021	0.165
Residuals	47	0.270	0.006	NA	0.525	NA
Total	50	0.515	NA	NA	1.000	NA

Table S3. ANOVA results of a linear mixed model for the net photosynthesis. Degrees of freedom (df), F-values (F) and significance probability (Pr) were shown for main effects ('Site' and 'Days') and interaction.

	df	F	Pr(>F)
(Intercept)	1, 13	225.17	0.0000
Site	1, 5	10.41	0.0233
Days	1, 5	34.29	0.0021
Site:Days	1, 5	0.00	0.9482

Table S4. Fucoxanthin to Chlorophyll a ratios. In case that the several values for each specimen were provided in each study cited (Ref), the minimum, maximum and mean values (Min, Max and Mean) are shown. If single value was reported, the data was provided in the column of Mean.

Specimen	**Min**	**Max**	**Mean**	**Ref**
Himanthalia elongata			0.044	Seely (1972)
Undaria pinnatifida			0.077	Seely (1972)
Laminaria ochroleuca			0.099	Seely (1972)
Laminaria saccharina			0.452	Seely (1972)
Sargassum muticum			0.464	Seely (1972)
Fucus distichus			0.407	Seely (1972)
Macrocystis pyrifera	0.520	0.770	0.645	Colombo-Pallotta et al (2006)
Macrocystis pyrifera	0.221	0.671	0.483	Marambio et al (2017)
Dictyopteris australis			0.064	Verna et al (2017)
Dictyota dicotoma			0.070	Verna et al (2017)
Labophora variegata			0.103	Verna et al (2017)
Padina tetrastromatica			0.121	Verna et al (2017)
Padina gymnospora			0.126	Verna et al (2017)
Spatoglossum asperum			0.141	Verna et al (2017)

Stoechospermum marginatum			0.070	Verna et al (2017)
Iyengaria stellata			0.158	Verna et al (2017)
Sargassum linearifolium			0.156	Verna et al (2017)
Carpomitra costata			0.010	Desmond et al (2019)
Carpophyllum flexuosum	0.010	0.480	0.245	Desmond et al (2019)
Cystophora platylobium			0.710	Desmond et al (2019)
Desmarestia ligulata	0.010	0.120	0.065	Desmond et al (2019)
Dictyota kunthii	0.350	0.510	0.420	Desmond et al (2019)
Ecklonia radiata	0.120	0.570	0.345	Desmond et al (2019)
Halopteris sp.			0.010	Desmond et al (2019)
Landsburgia quercifolia	0.640	0.890	0.777	Desmond et al (2019)
Macrocystis pyrifera	0.010	0.380	0.255	Desmond et al (2019)
Marginariella boryana	0.440	0.660	0.523	Desmond et al (2019)
Marginariella urvilliana	0.010	0.940	0.480	Desmond et al (2019)
Sargassum sinclairii			0.560	Desmond et al (2019)
Spatoglossum chapmanii	0.520	0.560	0.540	Desmond et al (2019)

Xiphophora gladiata	0.460	0.500	0.480	Desmond et al (2019)
Durvillaea antarctica	1.465	5.233	2.817	Mendez et al (2019)
Mean of Brown algae			0.372	
Diatom mat	0.567	0.956	0.657	Wulff et al (2008）
Diatom mat			1.655	Stief et al (2013
Diatom mat	0.509	1.768	1.000	Wulff et al (2005)
Diatom mat	0.950	1.770	1.360	Sundback et al (1996)
Mean of Diatom mat			1.168	